Scheme 1. Resolution and Stereoselective Synthesis of 25- and 26-Adamantyl-2-methylene-22,22,23,23-tetradehydro-19-norvitamin D Derivatives (4a, 4b, 5a, and 5b)

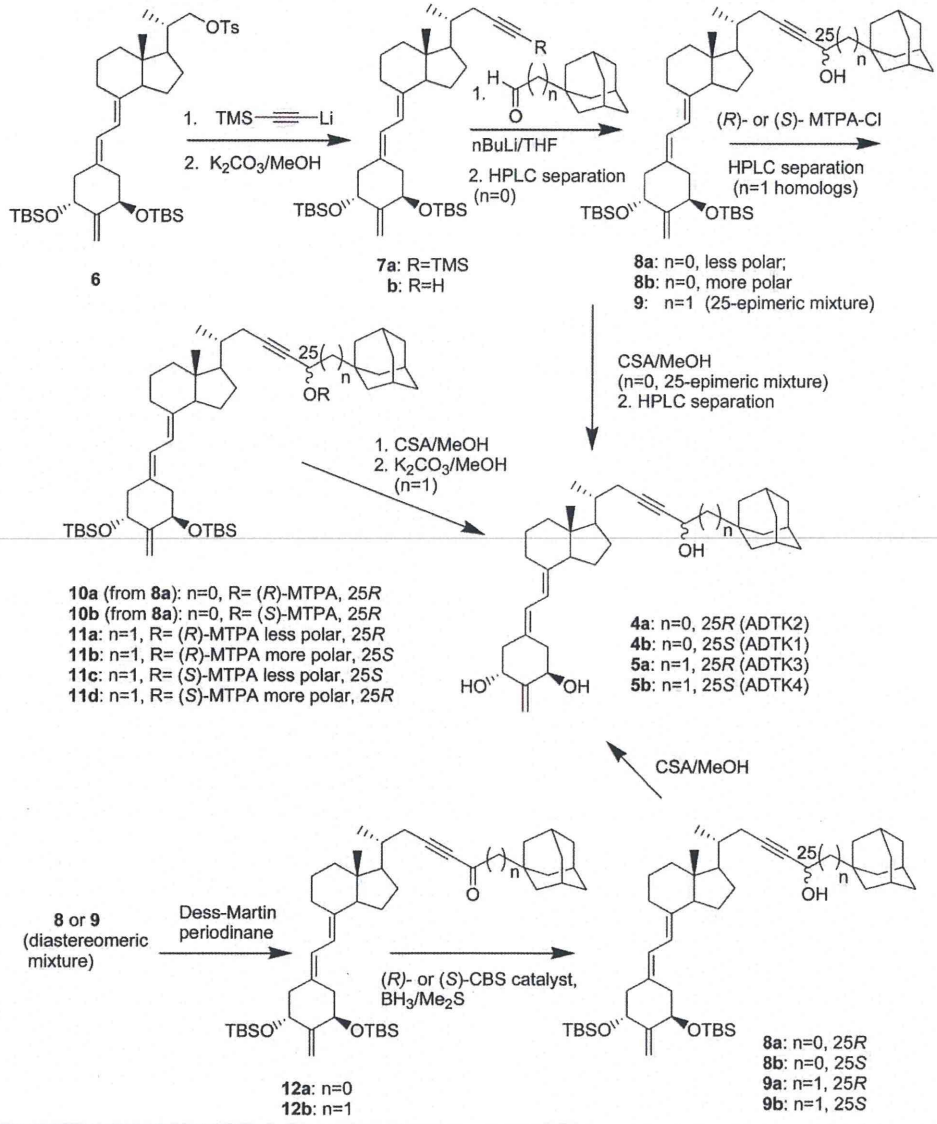

MeOH; (2) K_2CO_3, MeOH) yielded compound **5a** (ADTK3) (56%) and **11b** and **11c** gave **5b** (ADTK4, 67%).

Stereoselective Synthesis of ADTK1–4 (4b,a and 5a,b). The stereoselective syntheses of **4a,b** and **5a,b** were achieved by reduction of the 25-keto compounds **12a** and **12b** with a chiral oxazaborolidine catalyst.[15] The 25-hydroxyl compounds **8** and **9** were oxidized (Dess–Martin periodinane, DMP) to ketones **12a** (84%) and **12b** (68%), respectively, and selective reduction of the ketones was examined. Among several asymmetric catalysts, B-methyl-4,5,5-triphenyl-1,3,2-oxazaborolidine (BMTO)[15d] and Corey–Bakshi–Shibata catalyst (CBS),[15a–c] worked excellently. Reduction of **12a** with the (*R*)-BMTO catalyst in the presence of BH_3–SMe_2 (THF, 0 °C) gave the 25*R*-epimer **8a** in 70% yield with 78% de. Reduction of **12a** with the (*R*)-CBS catalyst (BH_3–SMe_2, THF, 0 °C) gave **8a** more selectively (91% de) in 86% yield. Reduction of **12a** with the (*S*)-CBS catalyst proceeded similarly to yield the 25*S*-epimer **8b** (87% de) in 75% yield. The *R*- and *S*-catalysts therefore showed the same stereoselectivities as previously reported.[15] Catalysts with the *R*-configuration gave the 25*R*-isomer **8a**, and with *S*-configuration yielded 25*S*-isomer **8b** with high selectivities. Selective reduction of **12b** with (*R*)- and (*S*)-CBS catalysts yielded **9a** and **9b**, respectively, with high selectivity and in good yields (>95% de 62% yield and >95% de 62% yield, respectively).

Determination of C(25) Stereochemistry of ADTK1–4 (4b,a and 5a,b) by ^{1}H NMR Spectroscopy. We determined the stereochemistry at C(25) of **4a**, **4b**, **5a**, and **5b** by using the new Mosher method.[16] Epimer **8a** of the 25-hydroxy compound was treated with (*S*)- and (*R*)-MTPA-chloride to give to (*R*)- and (*S*)-MTPA esters **10a** and **10b**, respectively. We also obtained pairs of (*R*)- and (*S*)-MTPA esters of the 26-adamantyl compound (**11a,b** and **11c,d**, respectively), as described above. We used one- and two-dimensional ^{1}H NMR spectra to identify the signals from protons in the side chain. The $\Delta\delta$ values (δ^S –

dx.doi.org/10.1021/jm401989c | J. Med. Chem. 2014, 57, 4073–4087

δ^R) of the protons on the side chains of three pairs of MTPA esters are shown in Chart 2C,D,E. The $\Delta\delta$ values of H-20 and

Chart 2. Determination of Stereochemistry at C(25) of Adamanty-19-norvitamin D Derivatives (4a,b and 5a,b) Using the New Mosher Method[a]

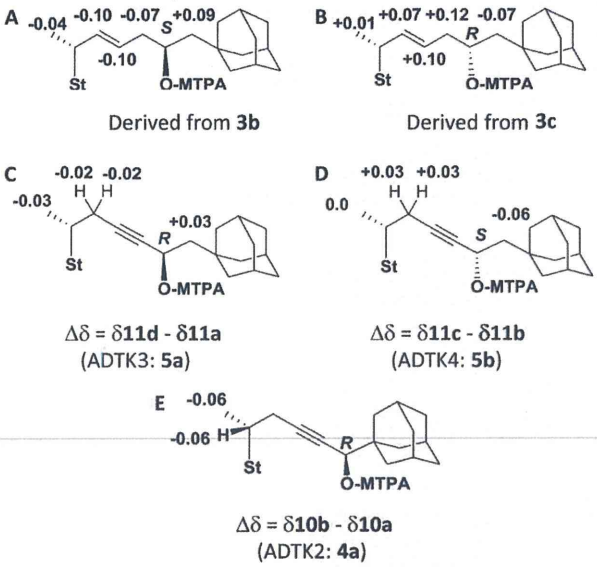

[a](A,B) Determination of the C(25) stereochemistries of adamantyl Δ^{22}-vitamin D compounds **3b** and **3c** as reported.[14a] Determination of the C(25) stereochemistries of **11a** and **11d** derived from ADTK3 (**5a**) (C), **11b** and **11c** derived from ADTK4 (**5b**) (D), and **10a** and **10b** derived from ADTK2 (**4a**) (E).

−21 (both −0.06) of **10a** and **10b** were correlated to the 25*R*-configuration, although the H-22 signals cannot be well assigned. Because the C(25) stereochemistry of **4b** (ADTK1), which was obtained by deprotection of **8b**, was confirmed to be *S* by X-ray crystallographic analysis of the rVDR complex (described below), the stereochemistries of **4a** and **4b** were confirmed to be *R* and *S*, respectively.

As shown above, we confirmed that **11a** (*R*-MTPA-ester) and **11d** (*S*-MTPA-ester) were converted to **5a**, and **11b** (*R*-MTPA-ester) and **11c** (*S*-MTPA-ester) to **5b**. The $\Delta\delta$ values δ(**11d**) − δ(**11a**) were −0.02, −0.02 (H22), −0.03 (H21), and +0.03 (H26), and accorded with the 25*R* stereochemistry (Chart 2C). The $\Delta\delta$ values δ(**11c**) − δ (**11b**) were +0.03 (H22), 0.0 (H21), and −0.06 (H26) and accorded with the 25*S* stereochemistry (Chart 2D). The stereochemistries of **5a** and **5b** were determined to be *R* and *S*, respectively, by X-ray crystal structural analysis of their rVDR complexes, as described below. All the stereochemistries at C(25) of the synthetic compounds **4a,b** and **5a,b** were therefore successfully determined using the new Mosher method. Chart 2 shows the present results compared with the corresponding results for our double-bond compounds (**3b** and **3c**).[14a]

Biological Activities of Adamantyl Vitamin D Compounds ADTK1−4 (4b,a and 5a,b). *VDR Affinity.* The VDR affinities of these vitamin D derivatives (**4a**, **4b**, **5a**, and **5b**) were determined based on competitive binding between [^{3}H]-1,25-$(OH)_2D_3$ and the substrate using recombinant hVDR-LBD.[17] The results are shown in Figure 1. The 25*S*-adamantyl compound **4b** had the highest activity, IC_{50} 0.5 nM, about 90%

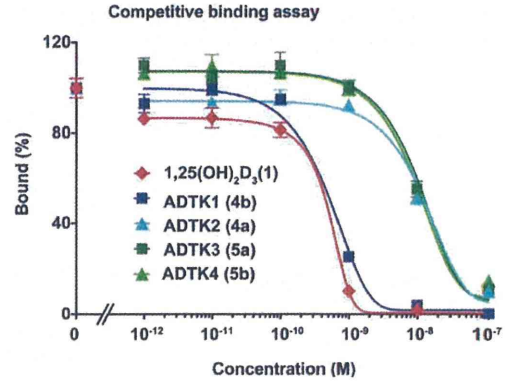

Figure 1. Competitive binding assays of adamantyl-19-norvitamin D derivatives **4a**, **4b**, **5a**, and **5b** compared with 1,25$(OH)_2D_3$ (**1**). hVDR-LBD expressed as glutathione S-transferase fusion protein was incubated with [^{3}H]-1,25$(OH)_2D_3$ in the presence of nonradioactive 1,25-$(OH)_2D_3$ (**1**) (red tilted square), **4a** (blue square), **4b** (cyan triangle), **5a** (green square), and **5b** (light green triangle) at a range of concentrations. All values represent means six standard deviations of triplicate assays.

that of 1,25$(OH)_2D_3$. The IC_{50}s of 25*R*-adamantyl (**4a**), 25*R*-(**5a**), and 25*S*-adamantyl (**5b**) longer side-chain compounds were 12, 13, and 12 nM, respectively.

Transcriptional Activity. VDR transactivation by ADTK1−4 (**4b,a** and **5a,b**) was evaluated using a luciferase reporter assay in human kidney cell lines (HEK293) transfected with mouse osteopontin vitamin D response elements (VDRE, SPP × 3-tk-LUC) and hVDR (pCMX hVDR) (Figure 2A).[14d] Compound **4b** had the highest activity (EC_{50} 0.07 nM, efficacy 81% that of the natural hormone) of the four compounds. The other compounds **4a**, **5a**, and **5b** had similar activities: EC_{50} (efficacy) **4a** 6.6 nM (38%), **5a** 1.5 nM (70%), and **5b** 1.1 nM (63%). It is worth noting that all the synthetic analogues have partial agonist activities in the transcriptional assay in HEK293 cells (Figure 2A). Their activation efficacies do not exceed that of 1,25-$(OH)_2D_3$ (**1**), even at doses 100 times higher. These compounds **4a**, **5a**, and **5b**, except for **4b**, inhibited weakly the transactivation induced by the natural hormone **1** (10 nM) (Figure 2B), while antagonist **3a** inhibited dose dependently the action of 1,25$(OH)_2D_3$.

Mammalian Two-Hybrid Assays. The effects of the adamantyl vitamin D compounds on the binding of VDR to various cofactors were evaluated by mammalian two-hybrid assays in HEK293 cells.[18] In these experiments, the effects of the ligands on VDR-retinoid X receptor α (RXRα) heterodimerization,[19,20] as well as VDR-coregulator binding including the steroid receptor coactivator 1 (SRC-1; or nuclear receptor coactivator 1 NCoA1),[21] nuclear receptor corepressor 1 (N-CoR),[22] and silencing mediator of retinoic acid and thyroid hormone receptor (SMRT or nuclear receptor corepressor 2, N-CoR2),[23] were evaluated by a luciferase reporter assay.[18] The results are shown in Figure 3.

Binding of VDR to RXRα. Ligand binding promotes heterodimerization of VDR with RXRα, which is essential for the VDR to recognize VDREs in the promoters of the target genes.[19,20] Adamantyl vitamin D **4b** activates (EC_{50} 0.6 nM) the VDR to bind to RXRα similarly to 1,25$(OH)_2D_3$ (EC_{50} 0.7 nM) (Figure 3A). The other compounds **4a** (EC_{50} 4.4 nM), **5a** (EC_{50} 2.3 nM), and **5b** (EC_{50} 0.8 nM) were a little less active than **4b**

dx.doi.org/10.1021/jm401989c | J. Med. Chem. 2014, 57, 4073−4087

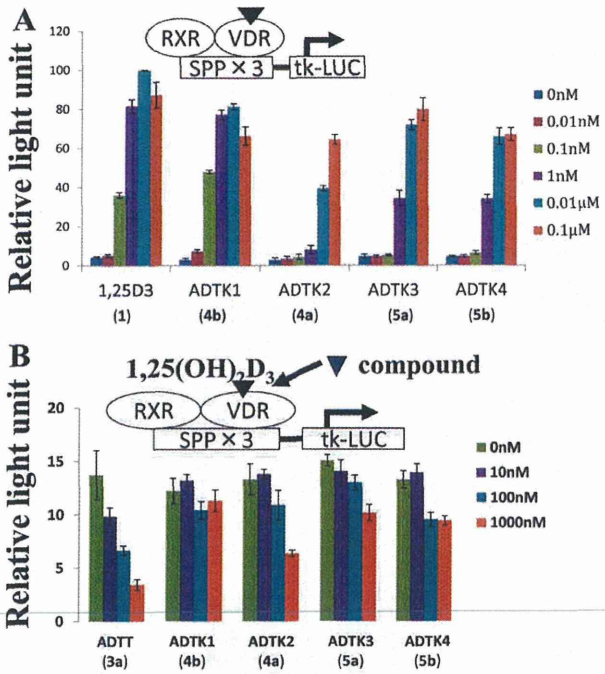

Figure 2. Transactivation of hVDR by adamantyl-19-norvitamin D derivatives **4a**, **4b**, **5a**, and **5b** compared with $1,25(OH)_2D_3$ (**1**). (A) HEK293 cells were cotransfected with TK-Spp × 3-LUC reporter plasmid and pCMX-VDR, and 8 h after transfection the cells were treated with several concentrations of **4a**, **4b**, **5a**, **5b**, and $1,25(OH)_2D_3$ (**1**). After 24 h, the cells were harvested for assaying luciferase and β-galactosidase activity using a luminometer (Molecular Devices, Sunnyvale, CA). (B) Antagonistic effect of vitamin D derivatives, **4a**, **4b**, **5a**, **5b**, and ADTT **3a**, on hVDR activated by $1,25(OH)_2D_3$ (**1**). HEK293 cells were cotransfected as in A and were treated with vitamin D derivatives (**4a**, **4b**, **5a**, **5b**, and **3a**) at a range of concentrations in the presence of $1,25(OH)_2D_3$ (**1**) (10 nM).

(Figure 3A). These results show that all analogues induce VDR-RXR binding.

Binding of VDR to SRC-1. SRC-1[21] directly binds to the activation function 2 (AF2) surface of nuclear receptors and stimulates the transcriptional activities in a hormone-dependent manner. This coactivator plays a central role in creating multisubunit coactivator complexes that act by participating in both chromatin remodeling and recruitment of general transcription factors.[21] The (25*S*)-adamantyl compound **4b** activated the binding of VDR to SRC-1 more strongly (EC_{50} 1.5 nM) than the natural hormone **1** did (EC_{50} 1.9 nM) (Figure 3B). The other compounds **4a** (EC_{50} 15.0 nM), **5a** (EC_{50} 6.5 nM), and **5b** (EC_{50} 13.5 nM) activated the VDR less potently. These results indicate that SRC-1 binds more strongly to the AF-2 surface of the VDR bound **4b** than that bound the natural hormone **1**.

Binding of VDR to N-CoR. N-CoR[22] mediates transcriptional repression and, as part of a complex, promotes histone deacetylation and the formation of repressive chromatin structures which may impede the access of basal transcription factors. Thus, **4b** dose-dependently inhibits binding of the VDR to N-CoR (EC_{50} 0.4 nM) slightly more potently than $1,25(OH)_2D_3$ does (EC_{50} 0.5 nM) (Figure 3C). The other analogues, **4a** (EC_{50} 4.0 nM), **5a** (EC_{50} 3.7 nM), and **5b** (EC_{50} 1.8 nM), inhibited binding of the VDR to N-CoR less potently than **4b**. The ability of adamantyl compounds to inhibit the binding of the

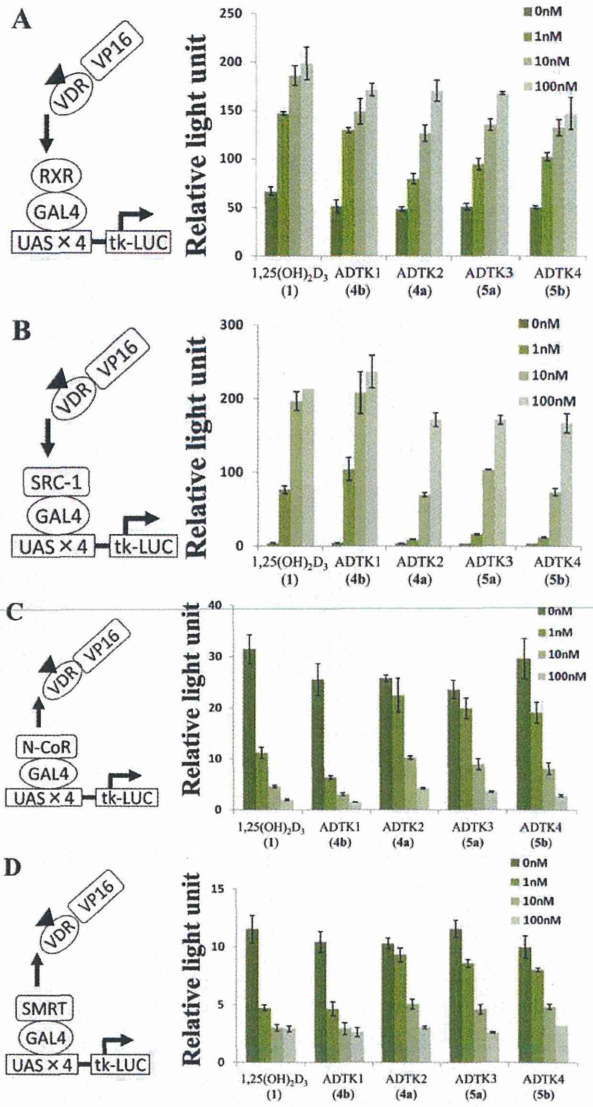

Figure 3. Effect of vitamin D derivatives **4a**, **4b**, **5a**, and **5b** on coactivator recruitment in a mammalian two-hybrid assay. (A) Effects of vitamin D derivatives on interaction between VDR and RXRα. HEK293 cells were cotransfected with CMX-GAL4-RXRα, CMX-VP16-VDR, and MH100(UAS) × 4-tk-LUC and treated with vitamin D compounds **4a**, **4b**, **5a**, **5b**, or $1,25(OH)_2D_3$ (**1**) at a range of concentrations. (B) Effects on interactions between VDR and SRC-1. HEK293 cells were cotransfected with CMX-GAL4-SRC-1, CMX-VP16-VDR, and MH100(UAS) × 4-tk-LUC and were treated with vitamin D compounds **4a**, **4b**, **5a**, **5b**, or $1,25(OH)_2D_3$ (**1**) at a range of concentrations. Effects on interactions of VDR with NCoR-1 (C) or SMRT (D). HEK293 cells were cotransfected with CMX-GAL4-N-CoR or CMX-GAL4-SMRT in combination with CMX-VP16-VDR and MH100(UAS) × 4-tk-LUC and were treated with vitamin D derivatives **4a**, **4b**, **5a**, **5b**, or $1,25(OH)_2D_3$ (**1**) at a range of concentrations.

two proteins is inversely proportional to the ability to activate binding of the VDR to SRC-1.

Binding of VDR to SMRT (NCoR2). The effect of **4b** (EC_{50} 0.5 nM) in inhibiting binding of the VDR to SMRT[23] was slightly less potent than that of $1,25(OH)_2D_3$ (EC_{50} 0.4 nM). Other analogues inhibited the binding of SMRT to the VDR less

dx.doi.org/10.1021/jm401989c | J. Med. Chem. 2014, 57, 4073−4087

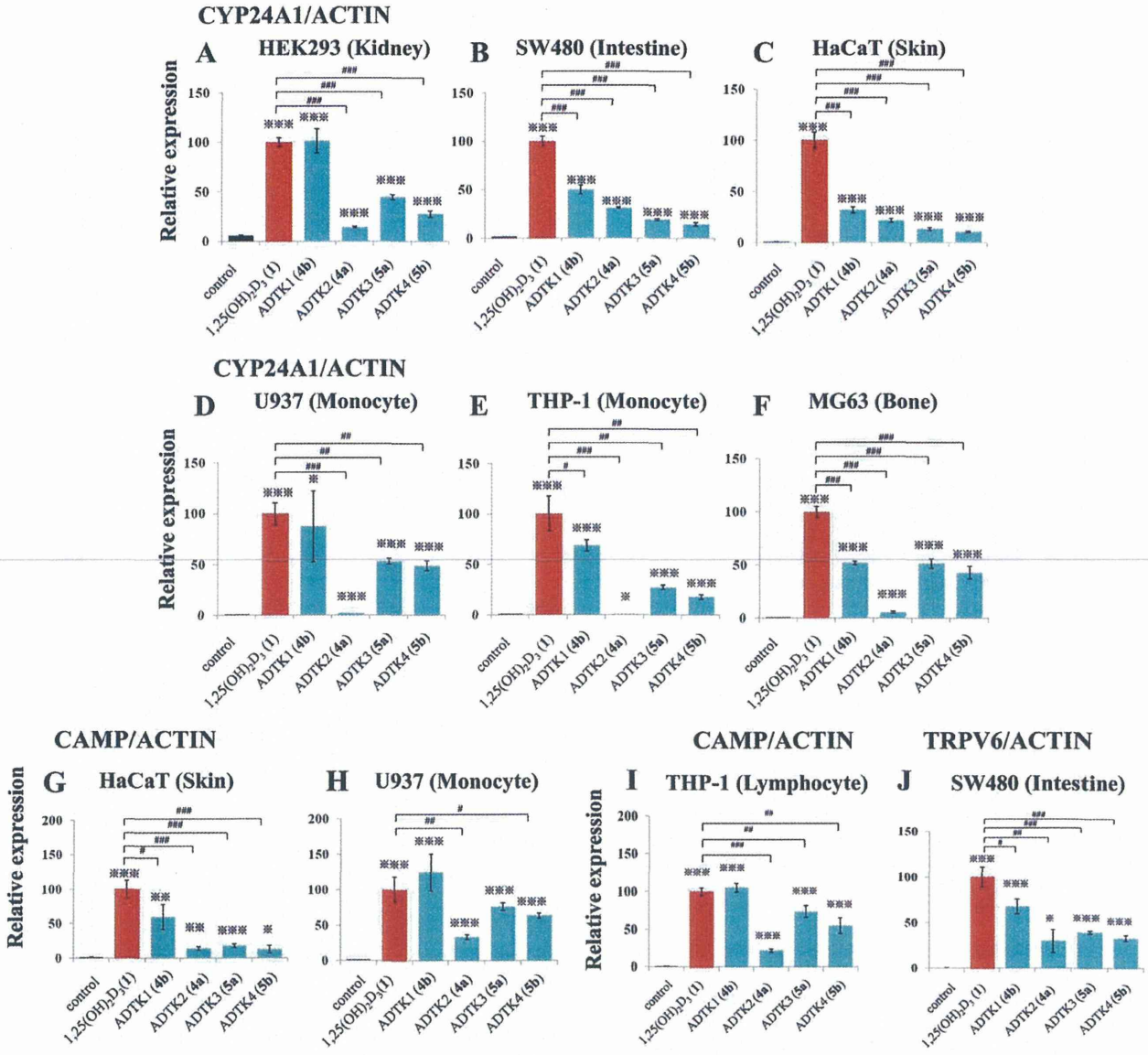

Figure 4. Effects of vitamin D derivatives **4a**, **4b**, **5a**, and **5b** on expression of CYP24A1 gene in kidney derived HEK293 (A), intestinal SW480 (B), keratinocyte HaCaT cells (C), monocyte-derived U937, (D), monocyte-derived THP-1 (E), and bone-derived MG63 (F) cells. Effects on the expression of CAMP gene in HaCaT (G), U937 (H), and THP-1 cells (I), and of TRPV6 gene in SW480 cells (J). Cells were treated with each sample (100 nM) for 24 h. *, $p < 0.05$; **, $p < 0.01$; ***, $p < 0.001$.

potently than **4b**: **4a** (EC_{50} 4.1 nM), **5a** (EC_{50} 2.4 nM), and **5b** (EC_{50} 2.8 nM) (Figure 3D).

Effect of Adamantyl Vitamin D Analogues on Endogenous Gene Expression in Various Cells. To examine the tissue-selective action of analogues **4a,b** and **5a,b**, we evaluated the expression of *CYP24A1*[24] gene in kidney-epithelium-derived HEK293, intestinal-mucosa-derived SW480, osteoblast-derived MG63, myeloid-derived THP-1 and U937, and skin-keratinocyte-derived HaCaT cells. We also examined the effect of the analogues on the expression of other genes, such as cathelicidin antimicrobial peptides (*CAMP*)[25] in THP-1, U937, and HaCaT cells, and transient receptor potential vanilloid 6 (*TRPV6*)[26] in SW480 cells. In all the experiments, we used equal concentrations (100 nM) of the ligands (**1**, **3a,b**, and **4a,b**).

CYP24A1. CYP24A1 is an enzyme[24] that inactivates 1,25-$(OH)_2D_3$ and its precursor 25-hydroxyvitamin D_3 (25-OHD_3) by hydroxylating their 24-position to yield the corresponding 24-hydroxylated metabolites. Binding of the ligands to the VDR induces enzyme expression in all the target tissues. The 25*S*-adamantyl compound **4b** induced *CYP24A1* mRNA expression in HEK293 cells similarly to the natural hormone (Figure 4A). The other compounds, **4a**, **5a**, and **5b**, increased *Cyp24A1* mRNA expression by 15%, 45%, and 30% of the activity of the natural hormone.

Interestingly, cell-type-selective gene induction was observed. In intestinal SW480 and in bone MG63 cells, **4b** activated the *CYP24A1* gene with about 50% of the activity of the natural hormone (Figure 4B,F). In skin HaCaT cell, mRNA expression of *CYP24A1* was 30% (Figure 3C) and in blood U937 and THP-

dx.doi.org/10.1021/jm401989c | J. Med. Chem. 2014, 57, 4073−4087

Table 1. Data Collection and Refinement Statistics

ligand	ADTK1 (**4b**)	ADTK3 (**5a**)	ADTK4 (**5b**)
PDB ID	3VTB	3VTC	3VTD
X-ray source	KEK-PF BL-5A	KEK-PF BL-5A	KEK-PFAR NW12A
space group	C2	C2	C2
cell dimensions			
a, *b*, *c* (Å)	153.56, 43.20, 42.49	126.85, 45.73, 46.64	153.18, 43.90, 42.53
α, β, γ (deg)	90.00, 95.56, 90.00	90.00, 93.87, 90.00	90.00, 95.73, 90.00
resolution range (Å)	50.00−2.00	50.00−1.50	50.00−2.70
(outer shell)	(2.07−2.00)	(1.55−1.50)	(2.80−2.70)
no. of reflections	66943	147172	29041
unique reflections	19 104	43 106	7900
completeness (%)	97.3	96.8	98.6
(outer shell)	(99.9)	(83.3)	(99.0)
R_{merge}	0.042	0.041	0.061
(outer shell)	(0.249)	(0.182)	(0.311)
	Refinement Statistics		
resolution range (Å)	50.00−2.00	50.00−1.50	50.00−2.70
(outer shell)	(2.07−2.00)	(1.55−1.50)	(2.80−2.70)
R factor R_{free}/R_{work}	0.286/0.246	0.209/0.184	0.278/0.213
(outer shell)	(0.506/0.521)	(0.237/0.206)	(0.400/0.325)

1 cells, 70−90% that of the natural hormone (Figures 3D,E). The 25*R*-isomer **4a** showed a low but clearer cell type dependent activity differences: in U937 and THP-1 cells 1%, MG63 5%, HEK293 14%, HaCaT cells 22%, and SW480 32%. The longer side chain compounds **5a** and **5b** showed about 50% activity in bone (MG63) and monocyte (U937) cells but showed lower activities (10−30%) in monocyte (THP1), intestine (SW480), and skin (HaCaT) cells (Figure 4). These adamantyl compounds (**4a,b** and **5a,b**) therefore all have different tissue selectivities.

Cathelicidine Antimicrobial Peptide (CAMP). CAMP[25] is an innate antimicrobial peptide and its induction has been observed, for example, in myeloid cells, keratinocyte, and intestinal cell lines. The expressions of the *CAMP* gene by **4b** in the monocytic cell lines U937 and THP-1 and in keratinocyte HaCaT cells were increased compared with those of *CYP24A1* (85%, 70%, and 30%, respectively) to 125%, 105%, and 60%, respectively (Figure 4H,I,G). The 25-epimer **4a** showed lower activities in U937, THP-1, and HaCaT cells, 30%, 20%, and 15%, respectively. The longer homologues **5a** and **5b** had moderate activities in U937 cells, 75% and 65%, respectively, and in THP-1 cells 74% and 55%, respectively (Figure 4H,I). However, they showed much lower activities in HaCaT cells, 20% and 15%. Thus, **5a** and **5b** showed 3.5−4-fold higher activities in monocytic cells than in skin cells (Figure 4G).

Transient Receptor Potential Vanilloid 6 (TRPV6). TRPV6[26] is a membrane calcium channel that is responsible for the first step in calcium absorption in the intestine. Its expression by **4b** in intestinal SW480 cells (Figure 4J) was similar (65%) to the expression of the *CYP24A1* gene. The longer homologues **5a** and **5b** induced TRPV6 expression less strongly (40% and 35%, respectively) but twice as strongly as the *CYP24A1* gene. The activities of **4a** were similar (30%) for *TRPV6* and *CYP24A1*.

X-ray Crystal Structural Analysis of rVDR-LBD Complexed with ADTK1, ADTK3, and ADTK4 (4b, 5a, and 5b). X-ray crystallographic structural analyses are essential for investigating the structure−activity relationships of the target compounds (**4a,b** and **5a,b**). The rVDR-LBD bound to **4b**, **5a**, and **5b** were crystallized as ternary complexes with a peptide containing LXXLL motif derived from VDR-interacting protein complex component DRIP205 (or MED1)[27] and analyzed to resolutions of 2.0, 1.5, and 2.7 Å, respectively (Table 1). The complex with **4a** (ADTK2) was also crystallized, but it was unstable to achieve good resolution (Supporting Information Figure S1, Table S1, and crystal data of rVDR-LBD/**4a**/DRIP). All of the complexes belonged to the space group C2. The root-mean-square deviations (rmsd) of the Cα atoms of the rVDR-LBDs complexed with **4b**, **5a**, and **5b** compared with the $1,25(OH)_2D_3$ complex (2ZLC)[28a] were 0.32, 0.56, and 0.38 Å, respectively. The complex with **5a** had the largest rmsd and was found to have somewhat a different unit cell structure (Supporting Information Figure S2) from the others, such as complexes with **4b** and **1** (2ZLC). Why does the complex with **5a** have a different unit cell structure? First, this might be a result of the positioning of the 25-hydroxyl group of **5a**. As shown in the overlay of the rVDR LBDs complexed with **5a** and **1** (2ZLC) (Figure 5A), the 25-hydroxyl group of **5a** takes a different position, which overlaps with the His393 of the complexes with **1**. Then the torsion angle (N−Cα−Cβ−Cγ) of His393 was changed significantly, from 170.7° of the complex with **1** to −72.1° of the complex with **5a**, which then caused the Cα positional changes of Thr302 (1.4 Å), Leu303 (2.5 Å), Glu304 (3.1 Å), and Leu305 (2.4 Å), as shown in Figure 5B. Interestingly, in **5b** complex, the positional shifts of Thr302 (1.1), Leu303 (0.7 Å), Glu304 (0.9 Å), and Leu305 (1.0 Å) are not as large as those of **5a** complex, and Leu303 and Glu304 are situated similarly to those of the complex with **1** (Figure 5C). In the VDR/**4b** complex, Leu303 and Glu304 interact with Ile134 (3.7 Å) and His130 (2.7 Å), respectively, of another VDR in the neighboring crystal unit (Supporting Information Figure S3A); this would stabilize the crystal packing. However, in the complex with **5a**, similar intercrystal-unit interactions are impossible because of the significant positional shifts of these residues (Supporting Information Figure S3B). In the complex with **5b**, the two residues, Leu303 and Glu304, are positioned similarly to **4b** and **1** rather than **5a** (Supporting Information Figure S3B).

The rVDR complexes of the ligands **4b**, **5a**, and **5b** all adopted the canonical active conformation (Supporting Information Figure S4). The side chain of the all ligands in the VDR adopted similar 16,17,20,22 dihedral angles directed toward the 21-methyl group of the natural hormone (Figure 5A,C): the

dx.doi.org/10.1021/jm401989c | J. Med. Chem. 2014, 57, 4073−4087

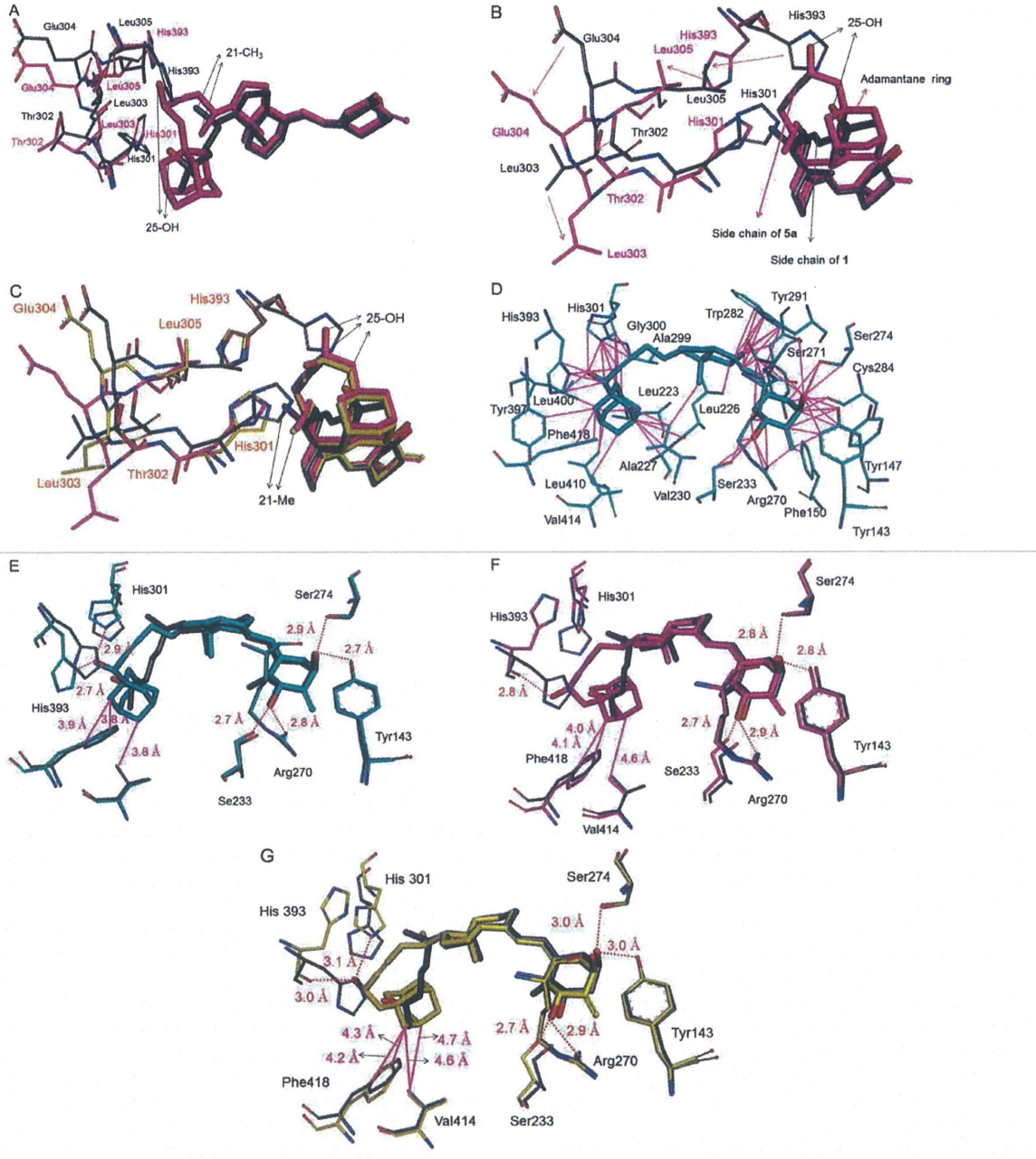

Figure 5. X-ray crystal structures of rVDR-LBD complexed with vitamin D compounds **4b**, **5a**, and **5b**. (A) Overlay of rVDR-LBD complexes with **5a** (magenta) and **1** (atom type). Residues His393 and His301-Leu305 are shown with narrow sticks. This view is shown focusing on the ligand structures. (B) Different view of the structures shown in (A) focusing on the residues His393 and His301-Leu305. (C) Overlay of rVDR-LBD complexes with **5a** (magenta), **5b** (yellow), and **1** (atom type). Residues His393 and His301-Leu305 are shown with the same color as the ligand. (D) van der Waals interactions (magenta line) of **4b** (atom type) with VDR residues (atom type) within 4 Å distance from **4b**. (E) Overlay of rVDR-LBD complexes with **4b** (cyan) and **1** (atom type). Hydrogen bonding interactions (red dotted lines) and van der Waals interactions with H12 residues (magenta) are shown. (F) Overlay of rVDR-LBD complexes with **5a** (magenta) and **1** (atom type). Hydrogen bonding interactions (red dotted line) and van der Waals interactions (magenta line) with H12 residues are shown. (G) Overlay of rVDR-LBD complexes with **5b** (yellow) and **1** (atom type). Hydrogen bonding interactions and van der Waals interactions with H12 residues are shown.

16,17,20,22-torsion angles of **4b**, **5a**, and **5b** were 54.5, 53.0, and 48.6°, respectively, whereas that of $1,25(OH)_2D_3$ was −44.3° and 16,17,20,21 dihedral angle was 77.2°. In these conformations, the terminal adamantane rings of **4b**, **5a**, and **5b** are placed around the 26,27-dimethyl group of **1**, and the other parts of the side chains occupy different positions from those in the natural hormone (Figure 5A,B,C).

The adamantane ring of **4b** interacts with as many as 10 residues within 4 Å, i.e., Leu223, Leu226, Ala227, and Val230 (H3), His301 (loop 6–7), Tyr397 and Leu400 (H11), Leu410

dx.doi.org/10.1021/jm401989c | J. Med. Chem. 2014, 57, 4073–4087

(loop11−12), and Val414 and Phe418 (H12) (Figure 5D). Most importantly, Phe418 and Vl414 of **4b** have closer contacts with the adamantane ring (both 3.8 Å) than the 26-methyl group of $1,25(OH)_2D_3$ (**1**) in all known VDR-LBD complexes: rat (both 4.3 Å), human (4.0 and 4.3 Å, respectively), and zebra fish (4.4 and 4.1 Å, respectively). Ligand **4b** in the VDR forms hydrogen bonds (2.7−2.9 Å) with the same six residues as the natural hormone (Figure 5E), but His301 and 393 adopt different conformations compared with the $1,25(OH)_2D_3$ complex (Figure 5E), although the Cα positional shifts are not large (0.6 and 0.4 Å, respectively). The methylene group at C(2) of **4b** interacts with Tyr143 (3.8 Å), Arg270 (3.5 Å), and Phe150 (4.0 Å) as does 2MD (Figure 5D). Phe418 in the complex of **4b** forms CH−π bonds with His393. All these data accord with **4b** having a high VDR affinity.

The complex of C(2S) epimer **4a** forms normal hydrogen bonds with Arg270 (2.8 Å), Ser274 (2.8 Å), and His393 (2.5 Å), weak hydrogen bonds with Trp143 (3.1 Å) and Ser233 (3.2 Å), and no hydrogen bond with His301 (4.6 Å) (Supporting Information Figure S1). The VDR therefore anchors **4a** more weakly than **4b**.

The complex with **5a** has the largest positional shifts at 301−306 (rmsd 1.8 Å) compared with the $1,25(OH)_2D_3$ complex (2ZLC) (Figure 5B). It was also noted that the positioning of DRIP peptide differs significantly (at the LXXLL part, rmsd 0.8 Å). The two A-ring hydroxyl groups form hydrogen bonds with Ser233, Arg270, Tyr143, and Ser274 (2.7−2.9 Å) (Figure 5F). The 25-hydroxyl group does not form hydrogen bond with the imidazole nitrogen of His393 but does with its main chain carbonyl group (2.8 Å); it forms no hydrogen bond with His301. The methylene group at C(2) interacts with the same residues Tyr143 (3.9 Å), Arg270 (3.5 Å), and Phe150 (4.0 Å) as **4b** does.

In the complex with rVDR-LBD, **5b** interacts similarly to **5a** except around C25. The 25-hydroxyl group forms weak hydrogen bonds with the imidazole nitrogen of His301 (3.1 Å) and the main chain carbonyl of His393 (3.0 Å) (Figure 5G). The C(2) methylene group of **5b** interacts differently from that of **5a** and 2MD: in addition to Tyr143 (3.9 Å), Arg270 (3.5 Å), and Phe150 (4.0 Å), Ser233 (3.9 Å) interacts with the CH_2 at a closer distance than that of **5a** complex (4.2 Å). Here, the difference in the side chain structure affects the conformations around the A ring too.

DISCUSSION

We have previously determined the crystal structures of the complex of rVDR bound to an antagonist/partial agonist **3a** (ADTT) [VDR affinity 80% of the natural hormone (**1**), transactivation EC_{50} 10^{-9} M (15% efficacy), inhibition of the transactivation of **1** (IC_{50} 3×10^{-9} M)] and the DRIP peptide. However, the VDR/**3a** complex adopts the active conformation.[14c] The rVDR complex with the one-carbon-longer analogue **3e** (ADMI4) [1/20 relative VDR affinity, transactivation EC_{50} 2.4×10^{-8} M (less than 10% efficacy), inhibition of the transactivation of **1** IC_{50} 3×10^{-8} M] also adopts the active form.[14c] *We thus confirmed that rVDR complexed with antagonists can adopt the active conformation in the crystal structure in the presence of the DRIP peptide.* We assumed that the DRIP peptide trapped the active conformation that exists as a minor conformation in solution (assuming 10−15% on the basis of the transactivation efficacy) by binding to its AF2 surface.

It is therefore not strange that the crystal structures of the rVDR-LBDs bound to the partial agonists **4b**, **5a**, and **5b** adopt the active conformations. The adamantane ring in all these compounds faces H12 (Figure 6A). We analyzed the interactions between the residues Phe418 and Val414 on H12 and the

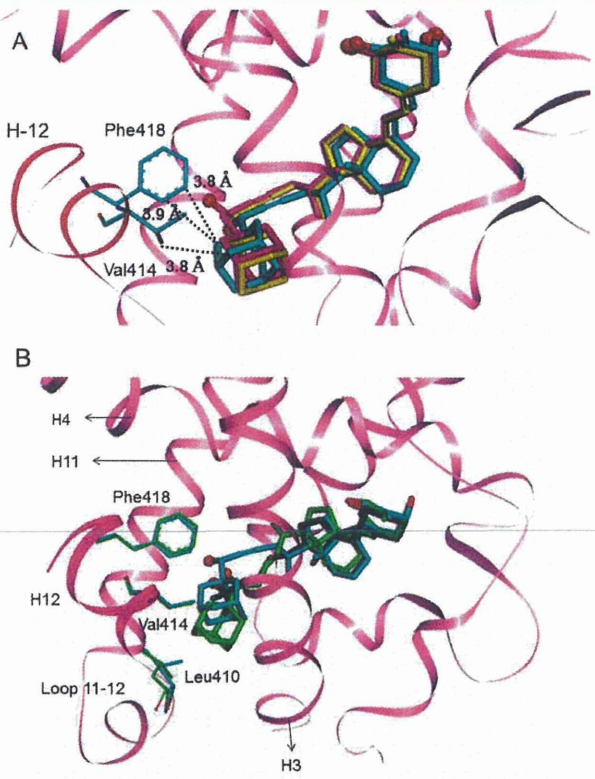

Figure 6. Interactions of adamantane ring with H12 residues in the rVDR-LBD complexes. (A) Overlay of rVDR complexes of **4b** (cyan), **5a** (magenta), and **5b** (yellow). The protein of **4b** complex is shown with pink ribbon with H12 magenta. Interaction of **4b** with the H12 residues, Phe418 and Val414, are shown with black dotted lines. The interactions of other ligands with H12 residues are shown in Table 2. (B) Overlay of the complexes with partial agonist **4b** (cyan), antagonist **3a** (green), and natural hormone **1** (atom type). The protein of **4b** complex is shown with a pink ribbon with H12 in magenta and three residues, Fe418, Val414 and Leu410, interacting with the adamantane ring of the ligands are shown.

adamantane ring of the ligands (**4a**, **5a**, and **5b**) in detail and compared them with those of other known VDR ligands (Table 2). It seems that H12 binds more tightly to the adamantine ring of **4b** than the 26-methyl group of $1,25(OH)_2D_3$, as shown by the distance between the two residues and side chain terminals of the ligands (Table 2). The distances between Phe418(422) and Val414(418) and $1,25(OH)_2D_3$ are equal to or longer than 4 Å in humans,[28c] rats,[28a,b] and zebrafish.[28d] The side chain terminal of the super agonist KH1060,[28e] which has a long side chain, is also in a similar region (Table 2, entry 10; Chart 1). However, the adamantine rings of ADTK1 (both 3.8 Å) and antagonist ADMI4 (3.5 and 4.0 Å) are at closer positions (Table 2). According to the equilibrium theory between active and inactive conformations,[14c,29] we assume that in solution these complexes would shift to an inactive form. It was reported for the zVDR complexes of 26,27-hexafluoro analogue CD578 (Chart 1; entry 13, Table 2) that the terminal fluorine atoms of the ligand are very close to Phe448 (3.6 Å), Val444 (3.5 Å), and Leu440 (3.3 Å), and these close interactions are correlated with the high potency of the

dx.doi.org/10.1021/jm401989c | J. Med. Chem. 2014, 57, 4073−4087

Table 2. Distances (Å) between H12 Residues with the Ligands in VDR

entry	VDR/ligand complexes (PDB code no.)	Phe418 (r),[a] 422 (h),[b] 448, (z)[c]	Val414 (r), 418 (h), 444 (z)
1	rVDR ADTK1 (**4b**) (3VTB)	3.8, 3.9	3.8
2	rVDR ADTK3 (**5a**) (3VTC)	4.0	4.60
3	rVDR ADTK4 (**5b**) (3VTD)	4.2, 4.3	4.8
4	rVDR ADTT (**3a**) (2ZMI)[14c]	4.5	4.3
5	rVDR ADMI4 (**3e**) (2ZMJ)[14c]	3.5	4.0
6	rVDR ADNY (**3f**) (2ZMH)[14c]	4.1, 4.2	4.4
7	rVDR-LBD/1,25(OH)$_2$D$_3$ (2ZLC)[28a]	4.3	4.3
8	hVDR-LBD/1,25(OH)$_2$D$_3$ (1DB1)[28c]	4.3	4.0
9	zVDR-LBD/1,25(OH)$_2$D$_3$ (2HC4)[28d]	4.4	4.1
10	hVDR-LBD/KH1060 (1IE8)[28e]	4.4	4.4, 4.0, 4.3
11	rVDR-LBD/2MD (1RJK)[28b]	4.1, 4.2	4.5
12	zVDR-LBD/CD578 (3DR1)[28f]	3.5	3.6

[a]Rat. [b]Human. [c]Zebrafish.

compound. However, these fluorine atoms interact directly with Phe422, with no intervening hydrogen atom. The F−C distance should be compared with (C)H−C distance, which is at least 1 Å shorter (3.0−3.3 Å) than the C(H)−C distance (4.0−4.3 Å). The positioning of the adamantane ring of **4b** is different from that of the double bond analogue **3a**, an antagonist, as shown in the VDR complexes (Figure 6B). The adamantine ring of **3a** in the VDR complex moves to the bottom of the protein to avoid crowding with Phe418 and Vl414 on H12. Furthermore, in the VDR, the vitamin D derivatives (**4** and **5**) with an adamantane ring and a triple bond have different side chain structures from those in the natural hormone (Figures 5A,B,C,E,F,G and 6B); this might be one reason why these compounds show different selectivities compared with the natural hormone.

CONCLUSIONS

Newly synthesized adamantyl vitamin D analogues (**4a,b** and **5a,b**) with a triple bond on the side chain are shown to be partial agonists. The adamantane rings of all the compounds face H12 and interact with Phe418 and Val414; furthermore, the side chain positioning differs significantly from that of the natural hormone (Figures 5A−C). The biological potencies of all the analogues are significantly high in terms of VDR affinity and transactivation (Figures 1 and 2). These compounds show significant selectivity in gene expressions in various cell types (Figure 4); for example, the activities of **4b** (ADTK1) in CYP24A1 gene expression in kidney, intestine, and bone were 1, 1/2, and 1/3, respectively, compared with the natural hormone. Similarly, CYP24A1 gene expressions of **5a** (ADTK3) in kidney, bone, and monocyte (U937) were significant for about 50% of the natural hormone but weak in skin (13%) and intestinal (19%) cells. ADTK2 (**4a**) showed selectivity in the expression of different genes; it showed no activity in the expression of CYP24A1 in monocyte U937 and THP-1 cells, but showed significant activities, 33% and 22%, respectively, in the expression of the CAMP gene in the same cells. The side chain structural differences between the 23-yne-adamantyl vitamin D compounds (**4b** and **5a,b**) and the natural hormone (Figures 5A−C) may be a reason why the former compounds showed significant cell-type selectivity. We are investigating further activities in in vivo expressions of various genes and also the effects on the elevation of calcium concentration and bone mineralization.

EXPERIMENTAL SECTION

Chemistry. All nonaqueous reactions were carried out under argon atmosphere in freshly distilled anhydrous solvents. We conducted high-pressure liquid chromatography (HPLC) by using Jasco PU-980 intelligent pumps equipped with an 801-SC solvent programmer and a Jasco UV-970 detector. All samples for biological assays were purified by HPLC and shown to have a purity of >95%. Columns used are YMC-Pack ODS-AM SH-342-5 (10 × 250 mm) or CHIRALPACK IE (4.6 mm × 250 mm). Nuclear magnetic resonance spectra were recorded in $CDCl_3$ solution on a Bruker Ultra Shield 400 MHz spectrometer (400 MHz for ^{1}H NMR and 100 MHz for ^{13}C NMR). Coupling constants are reported in hertz (Hz). Abbreviations used are singlet (s), doublet (d), triplet (t), quartet (q), and multiplet (m). Low-resolution mass spectra (MS) were obtained by electronic ionization on a Shimazu GCMSQP-2010NC PLUS 100 spectrometer at 70 eV, and m/z values are given with relative intensities in parentheses. High resolution mass spectra (HRMS) were obtained by JEOL JMS-T100LP with DART (direct analysis in real time). Ultraviolet spectra were recorded on a Hitachi U-3300 spectrometer.

1α-Hydroxy-2-methylidene-24-trimethylsilyl-23,23,24,24-tetradehydro-19,25,26,27-tetranorvitamin D$_3$ 1,3-Bis(*tert*-butyldimethylsilyl) Ether (7a). To a solution of trimethylsilylacetylene (282 μL, 2.03 mmol, 3 equiv) in anhydrous dioxane (3.0 mL) at 0 °C was added a 3.0 M hexane solution of MeLi (678 μL, 2.03 mmol, 3 equiv). The mixture was stirred at 0 °C for 30 min. To this mixture was added a dioxane (3.0 mL) solution of tosylate **6** (494.1 mg, 0.678 mmol), and then the mixture was heated in a sealed tube at 105 °C for 15 h. The reaction mixture was cooled to room temperature, a saturated NH_4Cl solution was added, and the mixture was extracted with ethyl acetate. The organic layer was washed with saline, dried over $MgSO_4$, and evaporated. The residue was chromatographed on silica gel (54 g) and eluted with 3% ethyl acetate/hexane to give **7a** (356.6 mg, 80%). **7a**: ^{1}H NMR ($CDCl_3$) d δ 0.02, 0.05, 0.06, 0.08 (each 3 H, s, OSiMe), 0.16 (9 H, s, $CSiMe_3$), 0.56 (3 H, s, 18-Me), 0.86, 0.90 (each 9H, s, $SiBu^t$), 1.09 (3H, d, J = 6.4 Hz, 21-Me), 4.41−4.45 (2H, m, H-1 and −3), 4.92, 4.97 (each 1H, s, C=CH_2), 5.84 (1H, d, J = 11.2 Hz, H-7), 6.21 (1H, d, J = 11.2 Hz, H-6). MS (EI) m/z (%): 654 (M+, 2), 522 (30), 450 (10), 366 (10), 234 (10), 73 (100).

1α-Hydroxy-2-methylidene-23,23,24,24-tetradehydro-19,25,26,27-tetranorvitamin D$_3$ 1,3-Bis(*tert*-butyldimethylsilyl) ether (7b). To a solution of **7a** (27.0 mg, 0.041 mmol) in THF/MeOH (1:0.7, 1 mL) was added K_2CO_3 (28.5 mg, 0.21 mmol, 5 equiv), and the mixture was stirred at room temperature for 24 h. After addition of a saturated solution of NH_4Cl, the mixture was extracted with ethyl acetate. The extract was washed with saline, dried over $MgSO_4$, and evaporated. The residue was chromatographed on silica gel (6.8 g) and eluted with 1% ethyl acetate/hexane to give **7b** (22.8 mg, 95%). **7b**: ^{1}H NMR ($CDCl_3$) δ 0.02, 0.06, 0.07, 0.08 (each 3 H, s, SiMe), 0.56 (3 H, s, 18-Me), 0.86, 0.90 (each 9 H, s, *t*-Bu), 1.09 (3 H, d, J = 6.4 Hz, 21-Me), 1.95 (1H, t, J = 2.4 Hz, terminal acetylene H), 4.41−4.45 (2 H, m, H-1 and -3), 4.92, 4.97 (each 1 H, s, C=CH_2), 5.84 (1 H, d, J = 11.2 Hz, H-7), 6.21 (1 H, d, J = 11.2 Hz, H-6). ^{13}C NMR ($CDCl_3$) δ −4.90, −4.86, 12.17, 18.16, 18.24, 19.09, 22.18, 23.36, 25.60, 25.78, 25.84, 27.53, 28.69, 30.90, 35.65, 38.58, 40.35, 45.58, 45.62, 47.62, 55.33, 56.16, 69.17, 71.63, 72.52, 83.36, 106.28, 116.25, 122.35, 132.91, 140.87, 152.96. MS (EI) m/z (%): 582 (M^+, 2), 450 (65), 366 (18), 351 (10), 234 (18), 73 (100). HRMS (DART) m/z calcd for $C_{36}H_{63}O_3Si_2$ (M^+ + OH) 599.432, found 599.427.

25-(1-Adamantyl)-1α,25-dihydroxy-2-methylidene-23,23,24,24-tetradehydro-19,26,27-trinorvitamin D$_3$ 1,3-Bis-(*tert*-butyldimethylsilyl) Ether (8). A 1.65 M hexane solution of *n*-BuLi (86 μL, 0.14 mmol, 2 equiv) was added to a solution of acetylene compound **7b** (41.0 mg, 0.07 mmol) at 0 °C, and 7 min later a solution of 1-adamantylformaldehyde (34.7 mg, 0.21 mmol, 3 equiv) in THF

(420 μL) was added. The mixture was stirred at 0 °C for 2 h, and then saturated NH_4Cl solution was added. The mixture was extracted with ethyl acetate, washed with saline, dried over $MgSO_4$, and evaporated. The residue was chromatographed on silica gel (4.7 g) and eluted with 5% ethyl acetate/hexane to give **8** (48.8 mg, 93%) as a mixture of diastereomers at C(25). The mixture was separated by HPLC [Hibar RT LiChrosorb Si 60 (7 μm), 10 mm × 250 mm, CH_2Cl_2/hexane 2/3, 4.0 mL/min] to give less polar **8a** and more polar **8b**. **8a** (more polar): ^{1}H NMR ($CDCl_3$) δ 0.02, 0.05, 0.06, 0.08 (each 3H, s, SiMe), 0.56 (3H, s, 18-Me), 0.86, 0.90 (each 9H, s, SiBu^t), 1.11 (3H, d, J = 6.4 Hz, 21-Me), 3.86 (1 H, s, H-25), 4.41−4.45 (2H, m, H-1 and −3), 4.92, 4.97 (each 1H, s, C=CH_2), 5.84 (1H, d, J = 11.2 Hz, H-7), 6.21 (1H, d, J = 11.2 Hz, H-6). MS m/z (%): 746 (M^+, 2), 614 (18), 596 (20), 366 (20), 234 (12), 135 (100), 73 (80). **8b** (less polar): ^{1}H NMR ($CDCl_3$) δ 0.02, 0.05, 0.07, 0.08 (each 3H, s, SiMe), 0.56 (3H, s, 18-Me), 0.86, 0.90 (each 9H, s, SiBu^t), 1.10 (3H, d, J = 2.4 Hz, 21-Me), 3.86 (1 H, s, H-25), 4.41−4.45 (2H, m, H-1 and −3), 4.92, 4.97 (each 1H, s, C=CH_2), 5.84 (1H, d, J = 11.2 Hz, H-7), 6.21 (1H, d, J = 11.2 Hz, H-6). MS m/z (%): 746 (M^+, 2), 614 (18), 596 (20), 366 (20), 234 (12), 135 (100), 73 (80).

26-(1-Adamantyl)-1α,25-dihydroxy-2-methylidene-23,23,24,24-tetradehydro-19, 27-dinorvitamin D_3 1,3-Bis(*tert*-butyldimethylsilyl) Ether (9). Similarly, one-carbon longer homologue **9** was synthesized from **7b** (6.4 mg, 0.011 mmol) and 1-adamantylacetaldehyde (5.88 mg, 0.033 mmol, 3 equiv). After chromatography on silica gel (1.1 g) with 1% ethyl acetate/hexane, **9** (5.3 mg, 80.4%) was obtained as a 1:1 mixture of C-25 epimers. **9**: ^{1}H NMR ($CDCl_3$) δ 0.02, 0.05, 0.06, 0.08 (each 3 H, s, SiMe), 0.55 (3 H, s, 18-Me), 0.86, 0.90 (each 9 H, s, SiBu^t), 1.06 (3 H, d, J = 8.0 Hz, 21-Me), 4.41−4.45 (2 H, m, H-1 and −3), 4.51 (1 H, m, 25-H), 4.92, 4.97 (each 1 H, s, C=CH_2), 5.84 (1 H, d, J = 11.2 Hz, H-7), 6.21 (1 H, d, J = 11.2 Hz, H-6). MS m/z (%): 760 (M+, 2), 610 (16), 475 (18), 366 (20), 234 (12), 135 (100), 73 (75).

25*R*-(1-Adamantyl)-1α,25-dihydroxy-2-methylidene-23,23,24,24-tetradehydro-19,26,27-trinorvitamin D_3 1,3-Bis-(*tert*-butyldimethylsilyl) Ether 25-[(*R*)-α-Methoxy-α-(trifluoromethyl)]-phenylacetate (10a). To a solution of 25-hydroxyl compound **8a** (2.3 mg, 3.1 μmol) in CH_2Cl_2 (400 μL) were added Et_3N (4.3 μL, 0.031 mmol, 10 equiv) and DMAP (2.1 mg, 0.017 mmol, 5.6 equiv). To this solution was added at 0 °C a solution of (*S*)-(+)-α-methoxy-α-(trifluoromethyl)]-phenylacetyl chloride (MTPA-Cl, 3.8 mg, 0.016 mmol, 5 equiv) in CH_2Cl_2 (250 μL) and stirred at the same temperature for 10 min and then at room temperature for 45 min. DMAP (2.8 mg, 0.023 mmol, 7.5 equiv) was added to the mixture and stirred further at room temperature for 2 h. Ice water was added to the reaction, and the mixture was extracted with ethyl acetate, and the extracts were washed with saline, dried over $MgSO_4$, and evaporated. The residue was chromatographed on silica gel to give **10a** (200 μg, 6.6%). **10a**: ^{1}H NMR ($CDCl_3$) δ 0.02, 0.05, 0.07, 0.08 (each 3 H, s, SiMe), 0.56 (3 H, s, 18-Me), 0.86, 0.90 (each 9 H, s, SiBu^t)), 1.10 (3 H, d, J = 6.4 Hz, 21-Me), 3.59 (3 H, s, OMe), 4.41−4.45 (2 H, m, H-1 and −3), 4.92, 4.97 (each 1 H, s, C=CH_2), 5.10 (1 H, s, H-25), 5.83 (1 H, d, J = 11.2 Hz, H-7), 6.21 (1 H, d, J = 11.2 Hz, H-6), 7.36−7.59 (5 H, m, phenyl).

(25*R*)-25-(1-Adamantyl)-1α,25-dihydroxy-2-methylidene-23,23,24,24-tetradehydro-19,26,27-trinorvitamin D_3 1,3-Bis-(*tert*-butyldimethylsilyl) Ether 25-[(*S*)-α-Methoxy-α-(trifluoromethyl)]- phenylacetate (10b). 25-Hydroxyl compound **8a** (3.0 mg, 4 μmol) was treated with (*R*)-(−)-MTPA-Cl to give (*S*)-MTPA ester (**10b**) (500 mg, 13%) similarly as above. **10b**: ^{1}H NMR ($CDCl_3$) δ 0.02, 0.05, 0.07, 0.08 (each 3H, s, SiMe), 0.56 (3 H, s, 18-Me), 0.86, 0.90 (each 9 H, s, SiBu^t), 1.05 (3 H, d, J = 6.4 Hz, 21-Me), 3.55 (3 H, s, OMe), 4.41−4.45 (2 H, m, H-1 and −3), 4.92, 4.97 (each 1 H, s, C=CH_2), 5.06 (1 H, s, H-25), 5.83 (1 H, d, J = 11.2 Hz, H-7), 6.21 (1 H, d, J = 11.2 Hz, H-6), 7.36−7.59 (5H, m, phenyl).

26-(1-Adamantyl)-1α,25-dihydroxy-2-methylidene-23,23,24,24-tetradehydro-19,27-dinorvitamin D_3 1,3-Bis(*tert*-butyldimethylsilyl) Ether 25-[(*R*)-α-Methoxy-α-(trifluoromethyl)]- phenylacetate (11a and 11b). 26-Adamantyl-25-hydroxyl compound **9** (5.2 mg, 6.8 μmol) was allowed to react with (*S*)−(+)−MTPA-Cl (8.9 mg, 38 μmol, 5.6 equiv) in the presence of Et_3N (9.5 μL, 68 μmol, 10 equiv) and DMAP (5 mg, 38 μmol, 5.6 equiv) similarly to the above experiments. After work-up and chromatography on silica gel (5 g) with 2% ethyl acetate/hexane, (*R*)-MTPA ester **11** (5.4 mg, 81%) was obtained as a 1:1 mixture of epimers at C-25. The mixture was separated by HPLC [Hiber RT LiChrosorb Si 60 (7 μm), 250 mm × 10 mm, CH_2Cl_2/hexane 2/3 4.0 mL/min] to give less polar **11a** and more polar **11b**. **11a** (less polar): ^{1}H NMR ($CDCl_3$) δ 0.025, 0.05, 0.065, 0.08 (each 3 H, s, SiMe), 0.54 (3 H, s, 18-Me), 0.86, 0.90 (each 9 H, s, SiBu^t), 1.04 (3 H, d, J = 6.4 Hz, 21-Me), 1.56−1.71 (2 H, overlapping, H-26), 3.53 (3 H, s, OMe), 4.41−4.45 (2H, m, H-1 and -3), 4.92, 4.97 (each 1 H, s, C=CH_2), 5.60 (1 H, t, J = 6.4 Hz, H-25), 5.83 (1 H, d, J = 11.2 Hz, H-7), 6.21 (1 H, d, J = 11.2 Hz, H-6), 7.37−7.56 (5 H, m, phenyl). **11b** (more polar): ^{1}H NMR ($CCDCl_3$) δ 0.025, 0.05, 0.065, 0.08 (each 3H, s, SiMe), 0.54 (3 H, s, 18-Me), 0.86, 0.90 (each 9 H, s, SiBu^t), 1.03 (3 H, d, J = 6.4 Hz, 21-Me), 1.45−1.88 (2 H, overlapping, H-26), 3.53 (3 H, s, OMe), 4.41−4.45 (2 H, m, H-1 and −3), 4.92, 4.97 (each 1 H, s, C=CH_2), 5.60 (1 H, t, J = 6.4 Hz, H-25), 5.83 (1 H, d, J = 11.2 Hz, H-7), 6.21 (1 H, d, J = 11.2 Hz, H-6), 7.37−7.56 (5 H, m, phenyl).

26-(1-Adamantyl)-1α,25-dihydroxy-2-methylidene-23,23,24,24-tetradehydro-19,27-dinorvitamin D_3 1,3-Bis(*tert*-butyldimethylsilyl) Ether 25-[(*S*)-α-Methoxy-α-(trifluoromethyl)]- phenylacetate (11c and 11d). 26-Adamantyl-25-hydroxyl compound **9** (5.6 mg, 7.4 μmol) was allowed to react with (*R*)-(−)-MTPACl (9.6 mg, 41 μmol, 5.6 equiv) in the presence of Et_3N (10 μL, 74 μmol, 10 equiv) and DMAP (5 mg, 41 μmol, 5.6 equiv) similarly to the above experiments. After work-up and chromatography on silica gel (5 g) with 2% ethyl acetate/hexane, (*S*)-MTPA ester **11** (3 mg, 41%) was obtained as a 1:1 mixture of epimers at C-25. The mixture was separated by HPLC [Hiber RT LiChrosorb Si 60 (7 μm), 250 mm × 10 mm, CH_2Cl_2/hexane 2/3 4.0 mL/min] to give less polar **11c** and more polar **11d**. **11c** (less polar): ^{1}H NMR ($CDCl_3$) δ 0.025, 0.05, 0.065, 0.08 (each 3 H, s, SiMe), 0.54 (3 H, s, 18-Me), 0.86, 0.90 (each 9 H, s, SiBu^t), 1.04 (3 H, d, J = 6.4 Hz, 21-Me), 3.53 (3 H, s, OMe), 4.41−4.45 (2 H, m, H-1,3), 4.92, 4.97 (each 1 H, s, C=CH_2), 5.60 (1H, t, J = 6.4 Hz, H-25), 5.83 (1H, d, J = 11.2 Hz, H-7), 6.21 (1H, d, J = 11.2 Hz, H-6), 7.36−7.59 (5 H, m, phenyl). **11d** (more polar): ^{1}H NMR ($CDCl_3$) δ 0.025, 0.05, 0.065, 0.08 (each 3 H, s), 0.54 (3 H, s), 0.86, 0.90 (each 9 H, s), 1.03 (3 H, d, J = 6.4 Hz, 21-Me), 3.53 (3 H, s, OMe), 4.41−4.45 (2 H, m, H-1, 3), 4.92, 4.97 (each 1 H, s, C=CH_2), 5.60 (1 H, t, J = 6.4 Hz, H-25), 5.83 (1 H, d, J = 11.2 Hz, H-7), 6.21 (1H, d, J = 11.2 Hz, H-6), 7.38−7.56 (5 H, m, phenyl).

(25*R*)-25-(1-Adamantyl)-1α,25-dihydroxy-2-methylidene-23,23,24,24-tetradehydro-19,26,27-trinorvitamin D_3 (4a). The less polar **8a** (1.35 mg, 1.8 μmol) was treated with CSA (1.68 mg, 7.2 μmol, 4 equiv) in MeOH (500 μL) at room temperature for 3 h. Saturated $NaHCO_3$ solution was added to the reaction at 0 °C, the mixture was extracted with ethyl acetate, the extract was washed with saline, dried over $MgSO_4$, and evaporated. The residue was chromatographed on Sephadex LH-20 (1 g) and eluted with $CHCl_3$/hexane/MeOH 70/30/1 to give **4a** 880 μg, 94%). **4a** (ADTK2): ^{1}H NMR ($CDCl_3$) δ 0.57 (3 H, s, 18-Me), 1.10 (3 H, d, J = 6.4 Hz, 21-Me), 3.86 (1 H, s, H-25), 4.44−4.51 (2H, m, H-1, 3), 5.10, 5.11 (each 1H, s, C=CH_2), 5.89 (1H, d, J = 12 Hz, H-7), 6.36 (1H, d, J = 12 Hz, H-6). ^{13}C NMR ($CDCl_3$) δ 12.23, 19.41, 22.25, 23.45, 25.99, 27.47, 28.29, 28.94, 29.70, 35.73, 37.15, 37.50, 37.79, 38.15, 40.29, 45.70, 45.79, 55.32, 56.32, 70.71, 71.81, 71.93, 77.22, 80.26, 85.13, 107.77, 115.43, 124.20, 130.58, 143.13, 151.93. MS m/z (%): 518 (M^+, 10), 365 (10), 347 (10), 295 (10), 135 (100), 93 (25), 79 (25). HRMS (DART) m/z calcd for $C_{35}H_{50}O_3$ (M^+) 518.376, found 518.368.

(25*S*)-25-(1-Adamantyl)-1α,25-dihydroxy-2-methylidene-23,23,24,24-tetradehydro-19,26,27-trinorvitamin D_3 (4b). The more polar **8b** (1.07 mg, 1.4 μmol) was similarly treated with CSA (1.31 mg, 5.6 μmol, 4 equiv) in MeOH (700 μL) at room temperature for 3 h. After similar work-up, the residue was chromatographed on Sephadex LH-20 (1 g) and eluted with $CHCl_3$/hexane/MeOH 70/30/1 to give **4b** (683 μg, 91%). **4b** (ADTK1): ^{1}H NMR ($CDCl_3$) δ: 0.57 (3H, s, 18-Me), 1.10 (3H, d, J = 6.4 Hz, 21-Me), 3.86 (1H, d, J = 4 Hz, H-25), 4.46−4.50 (2H, m, H-1, 3), 5.10, 5.11 (each 1H, s, C=CH_2), 5.89 (1H, d, J = 12 Hz, H-7), 6.36 (1H, d, J = 12 Hz, H-6). ^{13}C NMR ($CDCl_3$) δ 12.23, 19.41, 22.25, 23.45, 25.98, 27.46, 28.30, 28.94, 29.70, 35.71, 37.15, 37.49, 37.80, 38.15, 40.29, 45.70, 45.79, 55.32, 56.32, 70.71, 71.81, 71.92, 77.21,

dx.doi.org/10.1021/jm401989c | J. Med. Chem. 2014, 57, 4073−4087

80.26, 85.13, 107.77, 115.43, 124.20, 130.58, 143.13, 151.94. MS *m/z* (%): 518 (M^+, 10), 365 (10), 347 (10), 295 (10), 135 (100), 93 (25), 79 (25). HRMS (DART) *m/z* calcd for $C_{35}H_{50}O_3$ (M^+) 518.376, found 518.366.

(25*R*)-26-(1-Adamantyl)-1α,25-dihydroxy-2-methylidene-23,23,24,24-tetradehydro-19,27-dinorvitamin D_3 (5a). To a solution of the less polar isomer of *R*-MTPA ester **11a** (1.03 mg, 1 μmol) in MeOH (500 μL)was added a solution of CSA (1.22 mg, 5.2 μmol, 5 equiv) in MeOH (200 μL) at 0 °C, and the mixture was stirred at room temperature for 3 h. Saturated $NaHCO_3$ solution was added at 0 °C, the mixture was extracted with ethyl acetate, and the extract was washed with saline, dried over $MgSO_4$, and evaporated. The residue was dissolved in MeOH (600 μL), K_2CO_3 (130 mg) was added, and the mixture was stirred at room temperature for 24 h. Saturated NH_4Cl solution was added to the reaction mixture at 0 °C, and the mixture was extracted with ethyl acetate. The extract was washed with saline, dried, and evaporated. The residue was chromatographed on Sephadex LH-20 (1 g) and eluted with $CHCl_3$/hexane/MeOH 70/30/1 to give **5a** (314 μg, 56%). **5a** (ADTK3): ^1H NMR ($CDCl_3$) δ 0.56 (3 H, s, 18-Me), 1.07 (3 H, d, *J* = 6.4 Hz, 21-Me), 4.45–4.53 (3 H, m, H-1,-3, and 25), 5.10, 5.11 (each 1 H, s, C=CH_2), 5.88 (1H, d, *J* = 11.2 Hz, H-7), 6.36 (1H, d, *J* = 11.2 Hz, H-6). MS *m/z* (%): 532 (M^+, 10), 429 (10), 361 (10), 309 (10), 135 (100), 93 (40), 79 (40). HRMS (DART) *m/z* calcd for $C_{36}H_{52}O_3$ (M^+) 532.392, found 532.373.

The more polar isomer of *S*-MTPA ester **11d** was similarly hydrolyzed to give **5a**.

(25*S*)-26-(1-Adamantyl)-1α,25-dihydroxy-2-methylidene-23,23,24,24-tetradehydro-19,27-dinorvitamin D_3 (5b). The more polar isomer of longer side chain (*R*)-Mosher ester **11b** (1.05 mg, 1.1 mmol) was deprotected similarly to the above experiment. After purification by Sephadex LH-20 (1 g) column chromatography, **5b** (383 μg, 67%) was obtained. **5b** (ADTK4): ^1H NMR ($CDCl_3$) δ 0.56 (3 H, s, 18-Me), 1.07 (3 H, d, *J* = 6.4 Hz, 21-Me), 4.45–4.53 (3 H, m, H-1, -3, and -25), 5.10, 5.11 (each 1 H, s, C=CH_2), 5.88 (1H, d, *J* = 11.2 Hz, H-7), 6.36 (1H, d, *J* = 11.2 Hz, H-6). MS *m/z* (%): 532 (M^+, 10), 429 (10), 361 (10), 309 (10), 135 (100), 93 (40), 79 (40). HRMS (DART) *m/z* calcd for $C_{36}H_{52}O_3$ (M^+) 532.392, found 532.368.

The less polar isomer of *S*-MTPA ester **11c** was similarly hydrolyzed to give **5b**.

25-(1-Adamantyl)-1α-hydroxy-2-methylidene-25-oxo-23,23,24,24-tetradehydro-19,26,27-trinorvitamin D_3 1,3-Bis(*tert*-butyldimethylsilyl) Ether (12a). To a solution of an epimeric mixture at C(25) of **8** (39.0 mg, 52 μmol) in CH_2Cl_2 (1.4 mL) was added Dess–Martin periodinane (DMP, 85.9 mg, 202 μmol, 4 equiv) and stirred at room temperature for 4 h. Saturated Na_2SO_3 solution was added to the reaction, and the mixture was extracted with CH_2Cl_2, and the extracts were washed with saline, dried over $MgSO_4$, and evaporated. The residue was chromatographed on silica gel to give **12a** (32.8 mg, 84%). **12a**: ^1H NMR ($CDCl_3$) δ 0.03, 0.05, 0.07, 0.08 (each 3 H, s, SiMe), 0.57 (3 H, s, 18-Me), 0.86, 0.90 (each 9 H, s, SiBu^t), 1.14 (3 H, d, *J* = 6.8 Hz, 21-Me), 4.40–4.45 (2 H, m, H-1 and -3), 4.93, 4.97 (each 1 H, s, C=CH_2), 5.85 (1 H, d, *J* = 11.2 Hz, H-7), 6.21 (1 H, d, *J* = 11.2 Hz, H-6). ^{13}C NMR ($CDCl_3$) δ −4.90, −4.85, 0.22, 12.17, 18.16, 18.24, 19.55, 22.17, 23.33, 25.78, 25.84, 26.40, 27.69, 27.91, 28.67, 35.60, 36.56, 38.12, 38.59, 40.42, 45.63, 46.73, 47.62, 55.49, 56.23, 71.63, 72.51, 77.20, 80.12, 94.57, 106.31, 116.40, 122.28, 133.11, 140.59, 152.93, 194.06. MS *m/z* (%): 745 (M^+, 1), 612 (36), 383 (10), 366 (20), 229 (100), 135 (30), 73 (50). HRMS (DART) *m/z* calcd for $C_{47}H_{77}O_4Si_2$ (M^+ + OH) 761.536, found 761.528.

26-(1-Adamantyl)-1α-hydroxy-2-methylidene-25-oxo-23,23,24,24-tetradehydro-19,27-dinorvitamin D_3 1,3-Bis(*tert*-butyldimethylsilyl) Ether (12b). To a solution of **9** (29.7 mg, 39 μmol) in CH_2Cl_2 (1.4 mL) was added DMP (46.7b mg, 110 μmol, 2.8 equiv), and the mixture was stirred at room temperature for 2.5 h. Saturated Na_2SO_3 solution was added to the reaction, and the mixture was extracted with CH_2Cl_2, and the extracts were washed with saline, dried over $MgSO_4$, and evaporated. The residue was chromatographed on silica gel to give **12b** (20.1 mg, 68%). **12b**: ^1H NMR ($CDCl_3$) δ 0.03, 0.05, 0.06, 0.08 (each 3 H, s, SiMe), 0.56 (3 H, s, 18-Me), 0.86, 0.90 (each 9 H, s, SiBu^t), 1.12 (3 H, d, *J* = 6.8 Hz, 21-Me), 2.15 (2 H, s, H-26), 4.40–4.46 (2 H, m, H-1 and -3), 4.92, 4.98 (each 1 H, s, C=CH_2), 5.84 (1 H, d, *J* = 11.2 Hz, H-7), 6.21 (1 H, d, *J* = 11.2 Hz, H-6). MS *m/z* (%): 759 (M^+, 2), 701 (3), 626 (40), 383 (10), 366 (30), 243 (30), 135 (100), 73 (50). HRMS (DART) *m/z* calcd for $C_{48}H_{79}O_4Si_2$ (M^+ + OH) 775.552, found 775.588.

Stereo Selective Reduction of 12a with (4*R*)-2-Methyl-4,5,5-triphenyl-1,3,2-oxazaborolidine. To a solution of 25-keto compound **12a** (6.1 mg, 8.2 μmol) in THF (10 μL) was added a solution of (*R*)-BMTO (4.0 mg, 13 μmol, 1.6 equiv) and borane–dimethyl sulfide complex (BMS, 10.0–10.2 M, 1.4 μL, 14 μmol, 1.7 equiv) in THF (25 μL) at 0 °C, and the mixture was stirred for 1 h. MeOH was added at 0 °C, and the mixture was evaporated. The residue was chromatographed on silica gel (4.7 g) and eluted with 5% ethyl acetate/hexane to give **8a** (4.3 mg, 5.8 μmol 70%, 78% de). **8a**: ^1H NMR ($CDCl_3$) δ 0.02, 0.05, 0.06, 0.08 (each 3 H, s, SiMe), 0.56 (3 H, s, 18-Me), 0.86, 0.90 (each 9 H, s, SiBu^t), 1.11 (3 H, d, *J* = 6.4 Hz, 21-Me), 3.86 (1 H, s, H-25), 4.41–4.45 (2 H, m, H-1 and −3), 4.92, 4.97 (each 1 H, s, C=CH_2), 5.84 (1 H, d, *J* = 11.2 Hz, H-7), 6.21 (1 H, d, *J* = 11.2 Hz, H-6). MS *m/z* (%): 746 (M^+, 2), 614 (18), 596 (20), 366 (20), 234 (12), 135 (100), 73 (80).

Stereo Selective Reduction of 12a with (*R*)-3,3-Diphenyl-1-methyltetrahydro-1*H*,3*H*-pyrrolo[1,2-*c*][1,3,2]oxazaborole. To a solution of 25-keto compound **12a** (4.4 mg, 5.9 μmol) in THF (20 μL) was added a solution of (*R*)-CBS (2.1 mg, 7.6 μmol, 1.3 equiv) and BMS (10.0–10.2 M, 0.8 μL, 8.0 μmol, 1.3 equiv) in THF (14 μL) at 0 °C, and the mixture was stirred for 50 min. MeOH was added at 0 °C, and the mixture was evaporated. The residue was chromatographed on silica gel (5.5 g) and eluted with 5% ethyl acetate/hexane to give **8a** (3.8 mg, 86%, and 91% de).

Stereo Selective Reduction of 12a with (*S*)-3,3-Diphenyl-1-methyltetrahydro-1*H*,3*H*-pyrrolo[1,2-*c*][1,3,2]oxazaborole. To a solution of 25-keto compound **12a** (23.6 mg, 32 μmol) in THF (100 μL) was added a solution of (*S*)-CBS (12.5 mg, 45 μmol, 1.4 equiv) and BMS (10.0–10.2 M, 4.5 μL, 45 μmol, 1.4 equiv) in THF (80 μL) at 0 °C, and the mixture was stirred for 50 min. After similar work-up, the residue was chromatographed on silica gel to give **8b** (17.8 mg, 75%, 87% de) and recovered **12a** (2.2 mg, 9.3%). **8b**: ^1H NMR ($CDCl_3$) δ 0.02, 0.05, 0.07, 0.08 (each 3 H, s, SiMe), 0.56 (3 H, s, 18-Me), 0.86, 0.90 (each 9 H, s, SiBu^t), 1.10 (3 H, d, *J* = 2.4 Hz, 21-Me), 3.86 (1 H, s, H-25), 4.41–4.45 (2 H, m, H-1 and −3), 4.92, 4.97 (each 1 H, s, C=CH_2), 5.84 (1 H, d, *J* = 11.2 Hz, H-7), 6.21 (1 H, d, *J* = 11.2 Hz, H-6). MS *m/z* (%): 746 (M^+, 2), 614 (18), 596 (20), 366 (20), 234 (12), 135 (100), 73 (80).

Stereo Selective Reduction of 12b with a (*R*)-3,3-Diphenyl-1-methyltetrahydro-1*H*,3*H*-pyrrolo-[1,2-*c*][1,3,2]oxazaborole. Similarly, one-carbon longer homologue **9a** (25*R*) was synthesized from **12b** (2.1 mg, 2.7 μmol) by reduction with (*R*)-CBS (2.2 mg, 7.9 μmol, 2.9 equiv) and BMS (10.0–10.2 M, 0.92 μL, 9.2 μmol, 3.4 equiv) in THF (180 μL). After chromatography on silica gel (6.0 g) with 5% ethyl acetate/hexane, **9a** (1.4 mg, 1.9 μmol, 68%, >95%de) was obtained. **9a**: ^1H NMR ($CDCl_3$) δ 0.02, 0.05, 0.06, 0.08 (each 3 H, s, SiMe), 0.55 (3 H, s, 18-Me), 0.86, 0.90 (each 9 H, s, SiBu^t), 1.06 (3 H, d, *J* = 8.0 Hz, 21-Me), 4.41–4.45 (2 H, m, H-1 and -3), 4.51 (1 H, m, 25-H), 4.92, 4.97 (each 1 H, s, C=CH_2), 5.84 (1 H, d, *J* = 11.2 Hz, H-7), 6.21 (1 H, d, *J* = 11.2 Hz, H-6). MS *m/z* (%): 760 (M^+, 2), 610 (16), 475 (18), 366 (20), 234 (12), 135 (100), 73 (75).

Stereo Selective Reduction of 12b with a (*S*)-3,3-Diphenyl-1-methyltetrahydro-1*H*,3*H*-pyrrolo[1,2-*c*][1,3,2]oxazaborole. Similarly, one-carbon longer homologue **9b** (25*S*) was synthesized from **12b** (2.1 mg, 2.7 μmol) by reduction with (*S*)-CBS (2.2 mg, 7.8 μmol, 2.8 equiv) and BMS (10.0–10.2 M, 0.92 μL, 9.2 μmol, 3.4 equiv) in THF (180 μL). After chromatography on silica gel (6.0 g) with 5% ethyl acetate/hexane, **9b** (1.3 mg, 1.7 μmol, 62%, >95% de) was obtained. **9b**: ^1H NMR ($CDCl_3$) δ 0.02, 0.05, 0.06, 0.08 (each 3 H, s, SiMe), 0.55 (3 H, s, 18-Me), 0.86, 0.90 (each 9 H, s, SiBu^t), 1.06 (3 H, d, *J* = 8.0 Hz, 21-Me), 4.41–4.45 (2 H, m, H-1 and -3), 4.51 (1 H, m, 25-H), 4.92, 4.97 (each 1 H, s, C=CH_2), 5.84 (1 H, d, *J* = 11.2 Hz, H-7), 6.21 (1 H, d, *J* = 11.2 Hz, H-6). MS *m/z* (%): 760 (M^+, 2), 610 (16), 475 (18), 366 (20), 234 (12), 135 (100), 73 (75).

Cell Lines and Cell Cultures. Human kidney HEK293 cells (RIKEN Cell Bank, Tsukuba, Japan) were cultured in Dulbecco's Modified Eagle's Medium (DMEM) containing 5% inactivated fetal